AD-A074 347 ARMY ARMAMENT RESEARCH AND DEVELOPMENT COMMAND ABERD--ETC F/G 20/11
SHOCK PROPAGATION IN THE THREE-DIMENSIONAL LATTICE. I. MODEL AN--ETC(U)
JUN 79 J D POWELL, J H BATTEH

UNCLASSIFIED ARBRL-TR-02174 SBIE-AD-E430295 NL

| OF |
AD
A074347

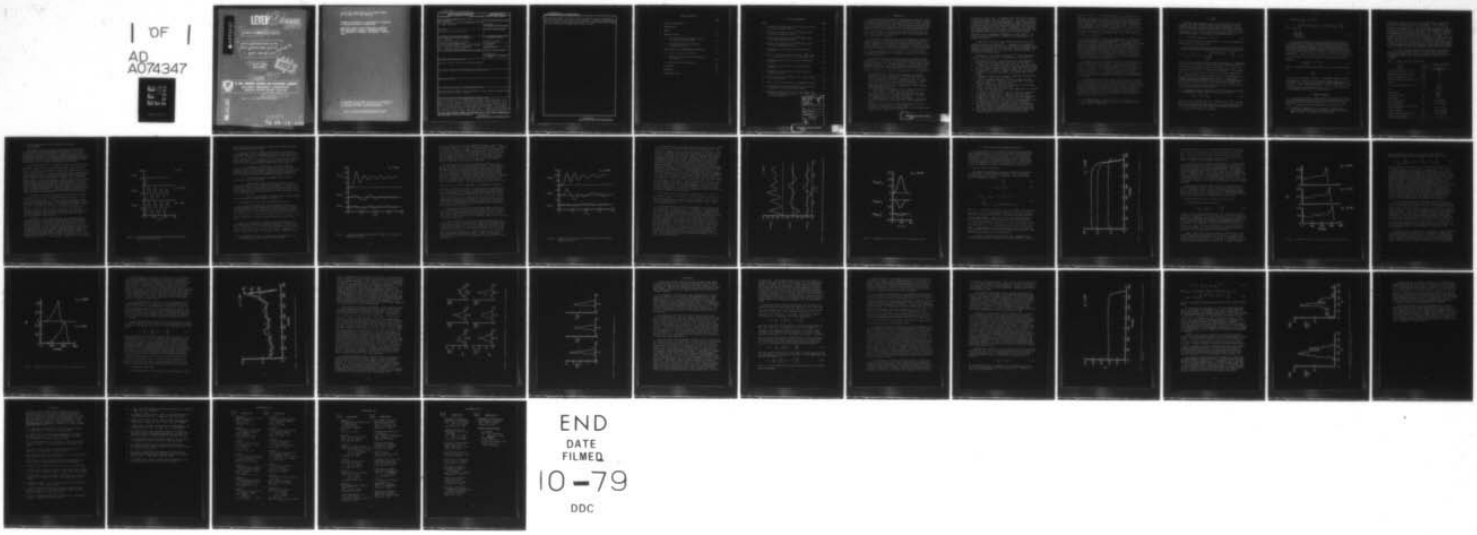

END
DATE
FILMED
10-79
DDC

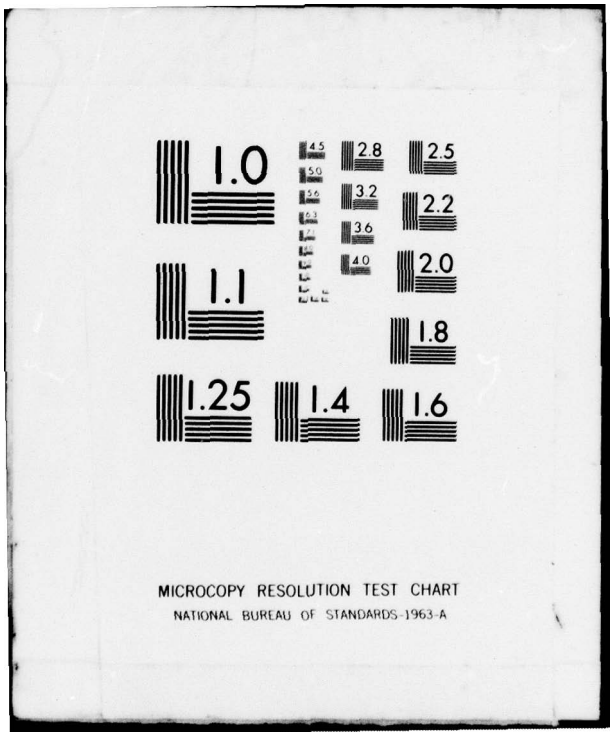
1.0
1.1
1.25
1.4
1.6
1.8
2.0
2.2
2.5
2.8
3.2
3.6
4.0
4.5
5.0
5.6
6.3
7.1
8.0
9.0
10.0
MICROCOPY RESOLUTION TEST CHART
NATIONAL BUREAU OF STANDARDS-1963-A

LEVEL II

TECHNICAL REPORT ARBRL-TR-02174

SHOCK PROPAGATION IN THE THREE-DIMENSIONAL LATTICE. I. MODEL AND RESULTS.

John D. Powell
Jad H. Batteh

June 1979

46 p.

US ARMY ARMAMENT RESEARCH AND DEVELOPMENT COMMAND
BALLISTIC RESEARCH LABORATORY
ABERDEEN PROVING GROUND, MARYLAND

1L161102AH43

Destroy this report when it is no longer needed.
Do not return it to the originator.

Secondary distribution of this report by originating or sponsoring activity is prohibited.

Additional copies of this report may be obtained from the National Technical Information Service, U.S. Department of Commerce, Springfield, Virginia 22161.

The findings in this report are not to be construed as an official Department of the Army position, unless so designated by other authorized documents.

The use of trade names or manufacturers' names in this report does not constitute indorsement of any commercial product.

UNCLASSIFIED

SECURITY CLASSIFICATION OF THIS PAGE (When Data Entered)

REPORT DOCUMENTATION PAGE		READ INSTRUCTIONS BEFORE COMPLETING FORM
1. REPORT NUMBER Technical Report ARBRL-TR-02174	2. GOVT ACCESSION NO.	3. RECIPIENT'S CATALOG NUMBER
4. TITLE (and Subtitle) SHOCK PROPAGATION IN THE THREE-DIMENSIONAL LATTICE. I. MODEL AND RESULTS		5. TYPE OF REPORT & PERIOD COVERED BRL Report 6. PERFORMING ORG. REPORT NUMBER
7. AUTHOR(s) John D. Powell and Jad H. Batteh		8. CONTRACT OR GRANT NUMBER(s)
9. PERFORMING ORGANIZATION NAME AND ADDRESS US Army Ballistic Research Laboratory ATTN: DRDAR-BLB Aberdeen Proving Ground, MD 21005		10. PROGRAM ELEMENT, PROJECT, TASK AREA & WORK UNIT NUMBERS RDT&E 1L161102AH43
11. CONTROLLING OFFICE NAME AND ADDRESS US Army Armament Research & Development Command US Army Ballistic Research Laboratory ATTN: DRDAR-BL, APG, MD 21005		12. REPORT DATE JUNE 1979 13. NUMBER OF PAGES 45
14. MONITORING AGENCY NAME & ADDRESS(if different from Controlling Office)		15. SECURITY CLASS. (of this report) Unclassified 15a. DECLASSIFICATION/DOWNGRADING SCHEDULE

16. DISTRIBUTION STATEMENT (of this Report)

Approved for public release; distribution unlimited.

17. DISTRIBUTION STATEMENT (of the abstract entered in Block 20, if different from Report)

18. SUPPLEMENTARY NOTES

19. KEY WORDS (Continue on reverse side if necessary and identify by block number)

Shock propagation, computer molecular dynamics, lattice dynamics, nonequilibrium phenomena, solitary waves, solitons.

20. ABSTRACT (Continue on reverse side if necessary and identify by block number) (hmn)

Shock propagation in a three-dimensional, monatomic, face-centered-cubic (FCC) lattice is studied using a computer-molecular-dynamic (CMD) technique. It is demonstrated that compression of the lattice gives rise to a spectrum of well-defined, longitudinal pulses (solitary waves) which propagate in the vicinity of the shock front amid the thermal background of the lattice. The properties of these pulses are examined in some detail and it is demonstrated that they are not completely stable. Rather, they tend to decay as they propagate into the lattice, producing both random, thermal motion and, in some cases, transverse

DD FORM 1 JAN 73 1473 EDITION OF 1 NOV 65 IS OBSOLETE

UNCLASSIFIED

SECURITY CLASSIFICATION OF THIS PAGE (When Data Entered)

solitary-wave motion. The effects of the solitary waves upon the temperature, density, and stress profiles and upon the approach to thermal equilibrium behind the shock front are investigated. Our results are compared with those of others and some indication of desirable future work is given.

TABLE OF CONTENTS

LIST OF ILLUSTRATIONS

I. INTRODUCTION

In a recent report[1] we discussed calculations performed on a model for simulating shock propagation in a one-dimensional, discrete lattice. The technique employed was to solve numerically the classical equations of motion of the atoms in the chain as they responded to the shock wave. From the solutions of the equations, one can then infer the macroscopic properties of the shock-compressed lattice by taking appropriate averages. This technique[2] is referred to as computer molecular dynamics and it is one of the few feasible methods for studying nonlinear, nonequilibrium, many-body problems.

In Reference 1 we emphasized that the one-dimensional calculations represented only an initial effort and that we intended to develop a computer program for solving the full three-dimensional problem. The present communication is the first in a series of two reports in which we will discuss the three-dimensional calculation. In the current work, we discuss the model very briefly and confine most of our attention to the significant results of the calculation. In the second report[3], the details of the calculation, including a discussion of the computer program, are presented.

The need for a microscopic, discrete-lattice treatment of shock propagation and its relevance to Army-related problems have been thoroughly discussed in Reference 1 and will not be discussed here. Before proceeding, however, it is perhaps worthwhile to indicate briefly some background on the three-dimensional problem and the rationale for our specific calculations. Three-dimensional CMD studies of shock propagation in crystal lattices have been undertaken by Tsai and coworkers[4-6]

---

1. J.D. Powell and J.H. Batteh, "Shock Propagation in the One-Dimensional Lattice", BRL Report No. 2009, US Army Ballistic Research Laboratories, Aberdeen Proving Ground, MD, 1977. See also J.H. Batteh and J.D. Powell, "Shock Propagation in the One-Dimensional Lattice at Nonzero Initial Temperature", J. Appl. Phys. 49, 3933 (1978) and J.H. Batteh and J.D. Powell, in Solitons in Action, edited by K. Lonngren and A. Scott (Academic Press, New York, 1978, p. 257.
2. B.J. Alder and T.E. Wainwright, "Studies in Molecular Dynamics. I. General Method", J. Chem. Phys. 31, 459 (1959).
3. J.D. Powell and J.H. Batteh, "Shock Propagation in the Three-Dimensional Lattice. II. Method of Calculation", BRL Report (to be published concurrently with this report).
4. R.A. MacDonald and D.H. Tsai, "Molecular Dynamical Calculations of Energy Transport in Crystalline Solids", Phys. Reports 46, 1 (1978).
5. D.H. Tsai and C.W. Beckett, "Shock Wave Propagation in Cubic Lattices", J. Geophys. Res. 71, 2601 (1966).
6. D.H. Tsai and R.A. MacDonald, "Second Sound in a Solid Under Shock Compression", J. Phys. C 6, L171 (1973).

over the last several years. An important and controversial conclusion of their work has been that the shock profile is not steady in time as is generally assumed in continuum calculations. Rather than observing a steady state, these workers concluded that the edge of the thermally equilibrated region behind the shock front propagates more slowly into the lattice than does the front itself. Consequently, the transition region between the front and the region of equilibrium grows with time. This anomalous behavior was explained by Tsai as being a natural extension of the low-temperature phenomenon of second sound[7,8]. For reasons discussed in Reference 1, however, this explanation is not entirely satisfactory.

In addition to the work of Tsai, similar calculations have been performed by Paskin and coworkers[9-11]. Although both investigators appear to obtain similar numerical data, substantial disagreement exists regarding the interpretation. In particular, Paskin has disputed Tsai's nonsteady interpretation; in fact, he claims essential agreement with the results of continuum models.

In Reference 1 and in other calculations[12-19], both analytic and numerical, shock propagation in a one-dimensional lattice has been

7. J.C. Ward and J. Wilks, "Second Sound and the Thermo-Mechanical Effect at Very Low Temperatures", Phil. Mag. 43, 48 (1952).
8. M. Chester, "Second Sound in Solids", Phys. Rev. 131, 2013 (1963).
9. A. Paskin and G.J. Dienes, "Molecular Dynamic Simulations of Shock Waves in a Three-Dimensional Solid", J. Appl. Phys. 43, 1605 (1972).
10. A. Paskin and G.J. Dienes, "A Model for Shock Waves in Solids and Evidence for a Thermal Catastrophe", Solid State Comm. 17, 197 (1975).
11. A. Paskin, A. Gohar, and G.J. Dienes, "Simulations of Shock Waves in Solids", J. Phys. C 10, L563 (1977).
12. J. Tasi, "Perturbation Solution for Growth of Nonlinear Shock Waves in a Lattice", J. Appl. Phys. 43, 4016 (1972). See also Erratum [J. Appl. Phys. 44, 1414 (1973)].
13. J. Tasi, "Perturbation Solution for Shock Waves in a Dissipative Lattice", J. Appl. Phys. 44, 2245 (1973).
14. J. Tasi, "Far-Field Analysis of Nonlinear Shock Waves in a Lattice", J. Appl. Phys. 44, 4569 (1973).
15. G.E. Duvall, R. Manvi, and S.C. Lowell, "Steady Shock Profile in a One-Dimensional Lattice", J. Appl. Phys. 40, 3771 (1969).
16. R. Manvi, G.E. Duvall, and S.C. Lowell, "Finite Amplitude Longitudinal Waves in Lattices", Int. J. Mech. Sci. 11, 1 (1969).
17. R. Manvi and G.E. Duvall, "Shock Waves in a One-Dimensional, Non-Dissipating Lattice", Brit. J. Appl. Phys. 2, 1389 (1969).
18. J.R. Hardy and A.M. Karo, "Theoretical Studies of Soliton-Like Behavior of Shocks in One-Dimensional Systems", LLL Report No. UCRL-79259, Lawrence Livermore Laboratory, Livermore, CA, 1977.
19. B.L. Holian and G.K. Straub, "Molecular Dynamics of Shock Waves in One-Dimensional Chains", Phys. Rev. B 18, 1593 (1978).

addressed. There is no doubt that the profile is nonsteady in one dimension and some investigators[1,12-14] have attributed the nonsteady behavior to the propagation behind the front of well-defined pulses called solitary waves. These pulses have been found to propagate at speeds which vary with amplitude and, thus, they tend to spread apart as they propagate. The spreading effect, then, gives rise to the nonsteady behavior observed in the calculations. The stability of the pulses was also studied[1] and they were found to be stable to within the numerical accuracy of the computer data. These stable pulses are referred to as solitons[20].

The extent to which solitary-wave propagation will significantly affect shock propagation (or other phenomena) in real three-dimensional crystals is not currently known. It is conceivable, for instance, that these well-defined pulses will not remain stable when they encounter oscillations transverse to their direction of propagation. In such a case one might expect that their influence upon the shock profile would, at most, be a transient effect in a three-dimensional model. Because of the importance of shock propagation to such Army-related problems as detonation, however, it is of obvious importance to settle the question conclusively as well as to check the general validity of the continuum approximations.

The purpose of the calculations carried out in this and the succeeding report is, therefore, twofold: First, we wish to determine the extent to which shock propagation in a three-dimensional discrete lattice is at variance with assumptions made in continuum models. Of particular interest is to determine whether solitary waves propagate in the lattice and, if so, their effects upon the shock profile. Second, we wish to develop an in-house capability for performing CMD calculations so that the technique can be applied to other problems of Army interest.

The organization of this first report is as follows. In Section 2 we describe the model under study, write down the equations of motion to be solved, and very briefly describe the method of solution. Details of the calculation are contained in Reference 3 which is devoted to that subject. In Section 3 the numerical results of the calculation are presented, and in Section 4 the shock profiles discussed. Finally, in Section 5 we discuss the results in greater detail and compare our calculations with those of other investigators. Some indication of possible future work is also given.

20. N.J. Zabusky and M.D. Kruskal, "Interaction of Solitons in a Collisionless Plasma and the Recurrence of Initial States", Phys. Rev. Letters 15, 240 (1965).

2. MODEL

The model whose properties we wish to study consists of a pure, monatomic, FCC lattice which is made as long as necessary in the z direction and which is periodic in the x and y directions. The periodicity in these directions is characterized by the integers L_x and L_y, respectively. Thus, for any function F which depends upon the velocities and displacements of the atoms in the lattice we have

$$F(x+\ell L_x a_o,\ y+mL_y a_o, z) = F(x,y,z) \tag{2.1}$$

where ℓ and m are arbitrary integers and a_o is the lattice constant or cube edge of the conventional cell.

The atoms will be assumed to interact via a Morse-type interatomic potential and therefore the Hamiltonian of the lattice can be written

$$H = 1/2 \sum_{i,j,k} \vec{V}^2_{ijk} + 1/2 \sum_{\substack{i,j,k \\ \ell,m,n}} \left[e^{-R(A_o|\vec{R}_{ijk}-\vec{R}_{\ell mn}|-1)} - 1 \right]^2 . \tag{2.2}$$

In Eq. (2.2) all quantities have been made nondimensional. H represents, of course, the total energy in the lattice and has been normalized by D, the dissociation energy of a single, isolated atom pair; $\vec{V}_{ijk}$ is the velocity of the $(ijk)^{th}$ atom, normalized by $\sqrt{D/m}$, where m is the atomic mass; $\vec{R}_{ijk}$ is the position vector of the $(ijk)^{th}$ atom, normalized by a_o; A_o is the lattice constant, normalized by r_o, the separation of an isolated atom pair at minimum potential; and R is a dimensionless parameter representing the degree of nonlinearity in the Morse potential. The sum over (ijk) runs over all atoms in the lattice and that over (ℓmn) is taken over all atoms in the vicinity of the $(ijk)^{th}$ for which the potential interaction is appreciable.

The equation of motion satisfied by the $(ijk)^{th}$ atom can be found in a straightforward manner from Eq. (2.2) and the result is

$$\ddot{\vec{R}}_{ijk} = 2\ R\ A_o\ \vec{F}_{ijk} \tag{2.3}$$

where $\vec{F}_{ijk}$ is the nondimensional force (normalized by $2\ RD/r_o$) exerted on the $(ijk)^{th}$ atom by the remaining atoms in the lattice and each dot represents differentiation with respect to the dimensionless time τ, i.e., the real time normalized by $\sqrt{m/D}\ a_o$.

Explicitly, $\vec{F}_{ijk}$ is given by

$$\vec{F}_{ijk} = \sum_{\ell,m,n} \left[e^{-2R(A_o |\vec{R}_{ijk}-\vec{R}_{\ell mn}|-1)} - e^{-R(A_o|\vec{R}_{ijk}-\vec{R}_{\ell mn}|-1)} \right] \times \frac{\vec{R}_{ijk}-\vec{R}_{\ell mn}}{|\vec{R}_{ijk}-\vec{R}_{\ell mn}|} \quad . \tag{2.4}$$

In all our calculations we will be concerned with solving Eqs. (2.3) numerically to determine the temporal evolution of the position and velocity of each atom in the lattice subject to some specific set of initial and boundary conditions. The initial conditions of each atom in the lattice are specified randomly, consistent with the assumption that prior to compression the lattice is in thermal equilibrium at temperature T. Thus, the probability that the α^{th} Cartesian component of $\vec{V}_{ijk}$ lies between V and V+dV is given by the Maxwellian distribution function

$$f = \left(\frac{\gamma}{2\pi}\right)^{1/2} e^{-\gamma V^2/2} \, dV \tag{2.5}$$

where γ is the ratio of the dissociation energy to the thermal energy, viz.,

$$\gamma = \frac{D}{k_B T} \tag{2.6}$$

and where k_B is Boltzmann's constant. The boundary condition applied to the model is such that the first plane of atoms normal to the z axis, located at z=0, is driven to the right at a constant nondimensional velocity U_p. This compression produces a shock wave propagating in the z direction and, from the solution of Eqs. (2.3), we infer the nature of the response of the lattice to the shock wave.

3. NUMERICAL RESULTS

In all our calculations we have assumed, unless otherwise noted, that the anharmonicity factor R in Eq. (2.2) was given by 6.29, a value which leads to a reasonable representation for a lattice of nickel atoms[21]. Furthermore, we have assumed that only atoms which were

21. F. Milstein, "Applicability of Exponentially Attractive and Repulsive Interatomic Potential Functions in the Description of Cubic Crystals", J. Appl. Phys. 44, 3825 (1973).

separated by a distance of unity or less (real distance normalized by a_o) exerted an appreciable force on one another. This assumption is equivalent to assuming that, in the equilibrium lattice at zero temperature, only an atom's first- and second-nearest neighbors contribute significantly to its potential interaction. The assumption was found to be reasonable for the currently used value of R. The lattice constant was then calculated (see Reference 3) and found to be 1.4034. The parameter γ was chosen to be 16 which corresponds to a lattice at roughly 150°K. The small value for the initial temperature was chosen so as to minimize the possibility of the lattice melting upon compression. Some calculations have also been done with γ=9, however, which corresponds to an initial temperature near room temperature, and no qualitative differences with results for the lower-temperature calculations were observed.

To assist in interpreting the results reported in the following sections, we have provided in Table I a list of symbols with their corresponding normalizing factors. The specific numerical values for the parameters used in our simulation of a nickel lattice are also included.

TABLE I. Symbols and Normalizing Factors.

Quantity	Symbol	Normalizing Factor or Numerical Value
Velocity of particle (i,j,k)	$\vec{V}_{ijk}$	$\sqrt{D/m}$
Nondimensional lattice constant	A_o	r_o
Position of particle (i,j,k)	$\vec{R}_{ijk}$	a_o
Potential energy of particle (i,j,k)	Φ_{ijk}	D
Density	ρ	ρ_o
Force exerted on particle (i,j,k)	$\vec{F}_{ijk}$	$2RD/r_o$
Time	τ	$\sqrt{m/D}\, a_o$
Stress tensor	$\overleftrightarrow{\sigma}$	$4D/a_o^3$
Compression velocity	U_p	$\sqrt{D/m}$
Temperature	θ	D/k_B
Dissociation energy	D	3.5×10^{-20} j
Mass of particle	m	9.7×10^{-26} kg
Equilibrium spacing for isolated pair of atoms	r_o	2.53×10^{-10} m
Lattice constant	a_o	3.52×10^{-10} m
Initial density ahead of shock	ρ_o	9.2×10^{28} m^{-3}
Nonlinearity parameter	R	6.29

3.1 The Initially Quiescent Lattice and the Existence of Solitary Waves.

The simplest instructive calculation that can be carried out is one for which the initial temperature of the lattice is zero ($\gamma \to \infty$). In that case each atom in the lattice is initially at rest in its equilibrium position and the shock wave produces motion only along the z direction. The effect of the shock wave can be determined most easily by plotting the velocity-time trajectories of various planes of atoms, normal to the z axis, as they are encountered by the shock.

A set of such trajectories is shown in Figure 1 for the case $U_p = 2.0$. Each plot is begun at time τ_o when the shock wave first excites the plane in question and the notation $\vec{V}_\alpha$ denotes the (common) velocity of atoms in the α^{th} plane. As can be seen from the figure the shock causes the second plane of atoms to move initially along an oscillatory-wave profile similar to that characteristic of atoms in a one-dimensional, harmonic chain[1]. As the wave propagates farther, however, and the atoms become farther displaced from their equilibrium positions, nonlinear effects become increasingly important. The nonlinearity of the lattice tends to steepen the wave profiles until such time as the nonlinear effect is exactly balanced by the dispersive effect of the lattice which tends to broaden the profile. At this time rather well-defined pulses known as solitary waves propagate in the vicinity of the shock front.

The evolution of the solitary waves can be seen in the velocity-time trajectories of the 20^{th} and 40^{th} planes in the figure. At the 20^{th} plane, the amplitudes of the pulses are seen to decrease as one moves away from the shock front. Since the pulse propagation velocity decreases with decreasing amplitude, a spreading effect ensues. Consequently, at the 40^{th} plane the pulses are seen to be slightly more distantly spaced than when the shock front was at the 20^{th} plane. As the pulses near the front propagate still farther into the lattice, it is found that their shapes remain essentially constant and they are then, by definition, solitary waves.

In Reference 1 we have shown that for a one-dimensional, Morse-potential lattice, solitary waves propagate near the shock front not only for the initially quiescent lattice, but also for the initially thermalized lattice. In the latter case, the solitary waves have varying amplitudes near the shock front and the spreading effect alluded to earlier prevents the shock profile from approaching a steady state. Furthermore, we have investigated the stability of the solitary waves in one dimension and found that, to within our numerical accuracy, they are stable to mutual collisions and to interaction with the thermal background of the lattice. One can expect, therefore, that the stability

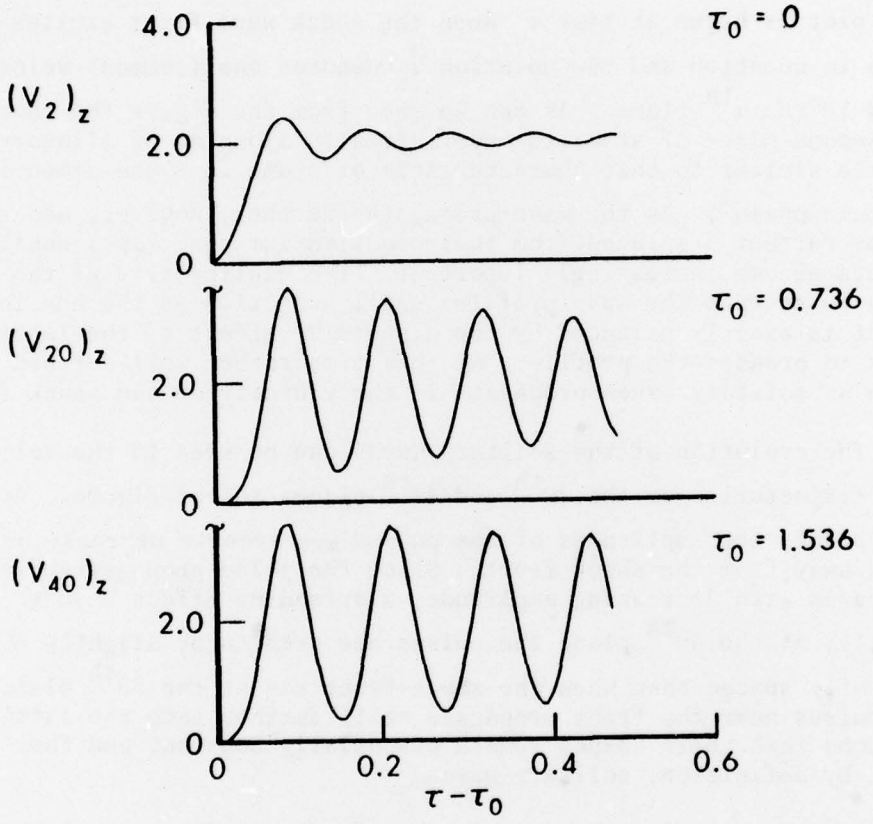

Figure 1. Evolution of solitary waves at the shock front in the initially quiescent lattice.

of the solitary waves will prevent the rapid establishment of thermal equilibrium behind the shock front.

It remains to determine whether similar effects occur when the three-dimensional, initially thermalized lattice is subjected to shock compression. Preparatory to this investigation, we have undertaken a rather thorough study[22] of the properties of solitary waves in the three-dimensional lattice. The principal conclusions of that study, which will be useful in interpreting the current work, are as follows.

1. Longitudinal solitary waves in a three-dimensional lattice are not so stable to mutual collisions as those in a one-dimensional chain, and the degree of stability decreases with increasing amplitude of the colliding pulses. Despite the lack of complete stability, however, the pulses do maintain their integrity fairly well.

2. The solitary waves are extremely stable to small, longitudinal, planar oscillations.

3. Longitudinal solitary waves are not stable to small, transverse, planar oscillations whenever the amplitude of the initial solitary wave is sufficiently large. Even in this case, however, most of the energy associated with the initial wave remains localized in the form of coupled longitudinal and transverse solitary waves which propagate at the same speed.

4. Solitary waves appear to be more stable to random thermal oscillations than to coherent planar oscillations.

3.2 Shock Propagation in the Initially Thermalized Lattice.

In an effort to determine how the shock profile is affected by thermal background in three dimensions, we have subjected an initially thermalized lattice to shock compression in the same manner as before. The compression velocity was again given by $U_p=2.0$ and the parameter γ was chosen to be 16. The periodicity of the lattice was given by $L_x=L_y=4$ which corresponds to 32 (unique) atoms in each plane normal to the z axis.

Again, it is instructive to plot velocity-time trajectories of individual planes, where now we define the velocity of a plane to be the average of the velocities of the atoms contained within the plane. Figure 2 shows such a trajectory for the 20^{th} plane subsequent to its being excited by the shock. From the plot of the z component, $(V_{20})_z$,

22. J.H. Batteh and J.D. Powell, "Solitary-Wave Propagation in the Three-Dimensional Lattice", Phys. Rev. B (in press).

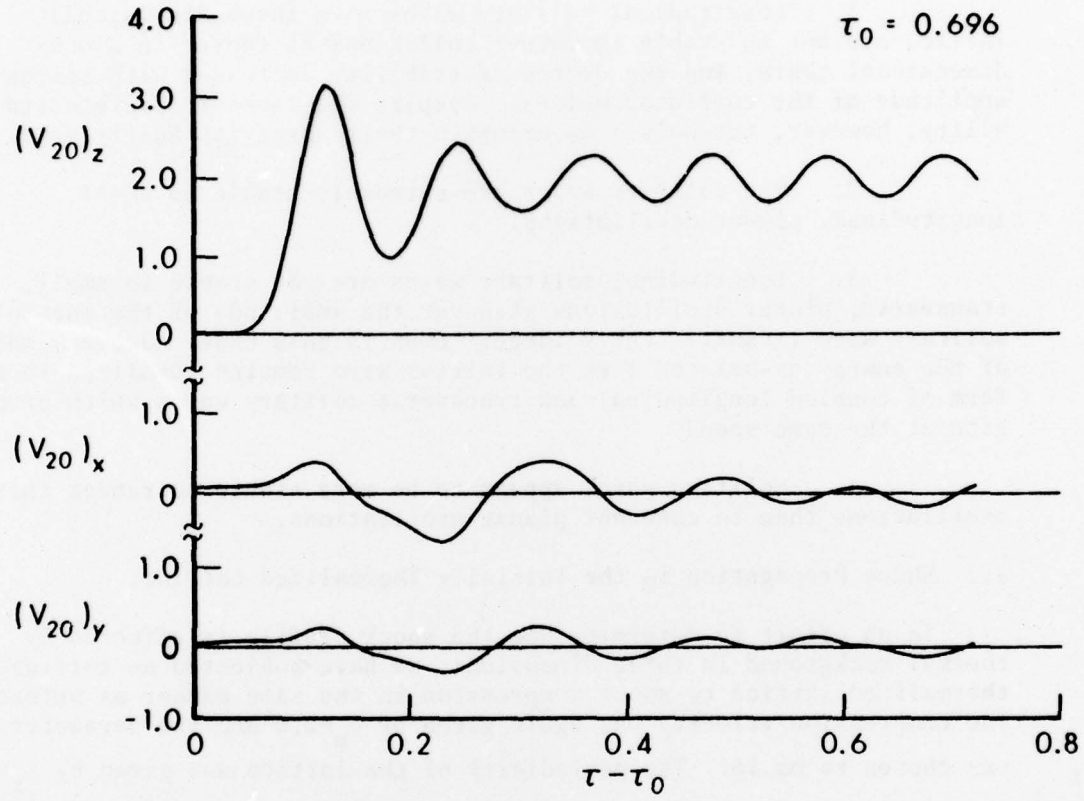

Figure 2. Velocity-time trajectory of the 20th plane in the initially thermalized lattice.

we can see that solitary waves are apparently forming in the vicinity of the shock front just as in the initially quiescent lattice. Comparing this figure with Figure 1, however, we observe that the amplitudes of the pulses are slightly less than in the quiescent lattice and the profiles are less well defined. The difference arises, no doubt, because in the thermalized lattice the solitary waves continuously interact with the thermal background of the lattice. It can also be observed that the shock front has given rise to some fairly large-amplitude planar oscillations in the transverse directions.

By the time the shock front has reached the 80^{th} plane in the lattice, the trajectory of which is shown in Figure 3, the profiles of the pulses near the front have become significantly more well defined. The amplitude of the leading pulse, however, has decreased by about 25%. It is conceivable that part of the energy associated with the original longitudinal solitary wave became coupled into the thermal background as this pulse propagated farther into the lattice. Apparently, however, a substantial part of the energy has been transferred to a rather well-defined planar oscillation in the x direction as can be seen in the plot of $(V_{80})_x$. This transverse pulse can also be seen in the plot of $(V_{20})_x$, but its amplitude is considerably less than when the front is near the 80^{th} plane. Since the pulse which propagates in the x direction seems to be exactly in phase with the leading longitudinal solitary wave, and travelling at the same propagation velocity, we are led to conclude that the two pulses are precisely the coupled solitary waves which we have observed in our previous work[22]. These coupled waves were found to arise whenever longitudinal solitary waves of sufficiently high amplitude encountered small, transverse planar oscillations. A similar pulse can be seen beneath the second longitudinal solitary wave in Figure 3.

It appears surprising that the coupled waves appear only in the x and z directions with little transfer of energy into the y direction. This unusual condition apparently arose because of the precise microscopic state of the lattice when the excitation occurred. At other times and in other calculations we have observed significant oscillations in all three directions.

We have allowed the shock front to propagate approximately 100 planes into the lattice discussed above. Because of the immense amount of computer time needed to solve all the equations of motion for such a large lattice, however, we have also repeated the calculation using a lattice for which $L_x=L_y=2$. This lattice contains 8 atoms per plane and, because of the smaller cross section, we were able to allow the shock to propagate considerably farther. In fact, in our longest calculations, the shock front has propagated more than 300 planes into the lattice.

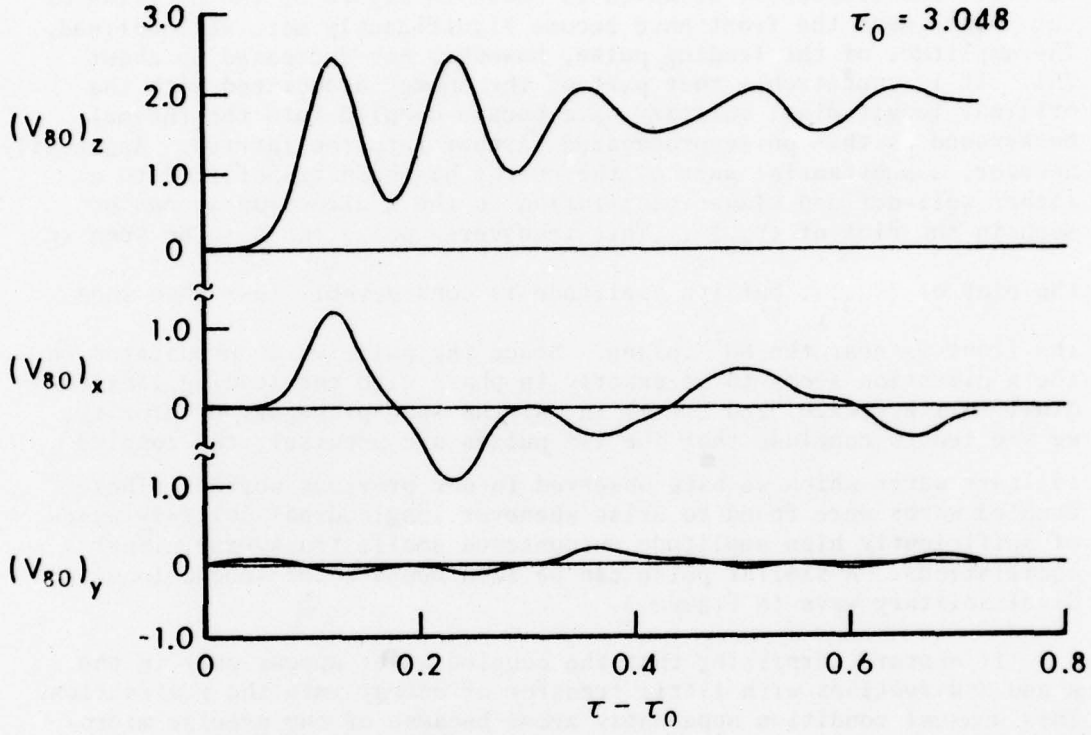

Figure 3. Velocity-time trajectory of the 80th plane in the initially thermalized lattice.

In Figure 4 we have shown the velocity-time trajectory of the 240^{th} plane of atoms for the shock calculation in the smaller lattice. The results are somewhat similar to those observed at the 80^{th} plane in the previous calculation except that the longitudinal wave profiles in the vicinity of the front are still more clearly defined and some of the energy has been transferred to the y direction. In fact, the leading longitudinal solitary wave appears to be accompanied by transverse solitary waves in both the x and y directions, but the shapes of the profiles are rather poorly defined because of interaction with the thermal background. In order to verify that the pulses we observe are indeed solitary waves, it is desirable to separate them from the thermal background. The separation can be accomplished most readily by a technique suggested in Reference 1. It was observed there that the high-amplitude solitary waves at the head of the shock front would propagate at a faster velocity than the rate at which thermal energy would diffuse into the lattice. Therefore, in order to separate the two effects, we instantaneously stopped the compression when the shock front had reached the 243^{rd} plane in the lattice. The atoms beyond the 243^{rd} plane, those in the uncompressed lattice, were then placed at rest in their equilibrium positions so that the hot, shock-compressed lattice was directly next to a cold lattice. One should then be able to observe the well-defined, high-amplitude solitary waves propagating into the cold lattice, leaving the thermal background behind.

The results of the calculation are shown in Figure 5. We have plotted the velocity-time trajectory of the 260^{th} plane in the lattice after the compression was stopped at the 243^{rd} plane. Three extremely well-defined pulses can be seen to propagate exactly in phase in the three Cartesian directions.

We have now observed solitary-wave propagation in the vicinity of the shock front in a number of cases. To summarize, our understanding of precisely how this phenomenon occurs is as follows. Subjecting the lattice to shock compression produces a spectrum of longitudinal solitary waves which propagate into the lattice and interact with the thermal background. When these solitary waves are subjected to transverse planar oscillations (however small) they accentuate those oscillations and, for sufficiently strong longitudinal waves, transverse solitary waves are generated. The transverse waves are coupled to the original wave and propagate in phase with it. The solitary waves, however, are not completely stable to the thermal oscillations in the lattice and one can expect that they will eventually decay as they propagate into the lattice. The energy which evolves as a result of the decay then increases the random thermal energy (temperature) behind the shock front. In the following section we will discuss the effects of solitary waves upon the shock profiles.

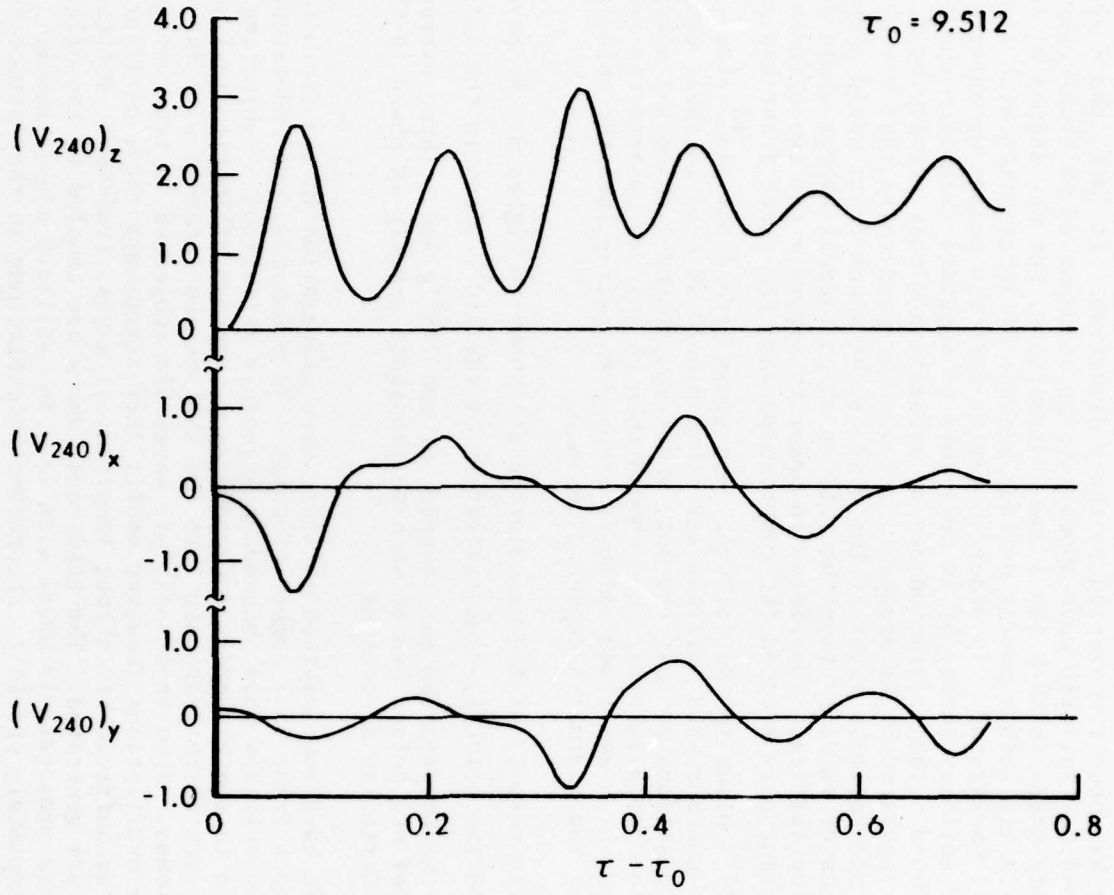

Figure 4. Velocity-time trajectory of the 240^{th} plane in the initially thermalized lattice.

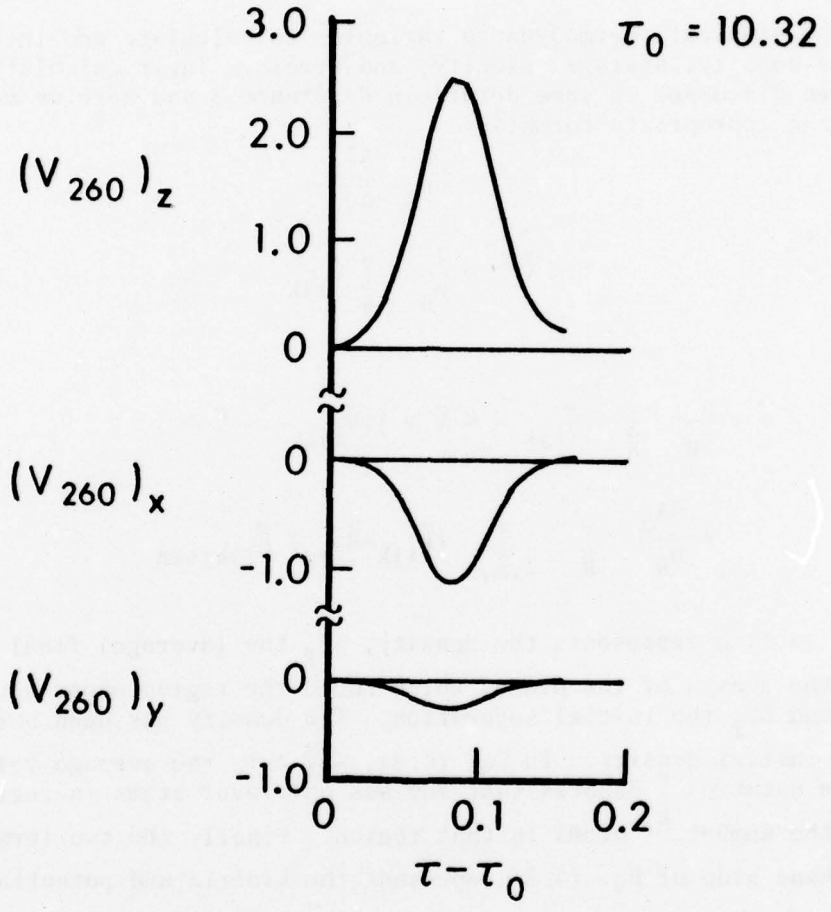

Figure 5. Propagation of solitary waves into the quiescent lattice.

4. SHOCK PROFILES AND THERMODYNAMIC QUANTITIES

In this section we wish to examine the shock profiles predicted from our numerical data. We will be particularly interested in determining how the propagation of solitary waves in the lattice affects these profiles. In calculating all profiles, we have averaged the thermodynamic variable in question over regions of the lattice which were microscopically large but macroscopically small. In most calculations the regions were chosen to be 16 planes in length (along the z axis) and contained, therefore, 128 atoms for the case $L_x=L_y=2$.

4.1 Density, Velocity, and Stress.

The simplest thermodynamic variables to calculate and interpret are the density, average velocity, and stress. Their calculation has been discussed in some detail in Reference 3 and here we merely quote the appropriate formulas:

$$\rho = \frac{\Delta Z_i}{\Delta Z_f} \tag{4.1}$$

$$\langle \vec{V} \rangle = \frac{1}{n_R} \sum_R \vec{V}_{ijk} \tag{4.2}$$

$$\begin{aligned} \overleftrightarrow{\sigma} = & \frac{\rho}{n_R} \sum_R (\vec{V}_{ijk} - \langle \vec{V} \rangle)(\vec{V}_{ijk} - \langle \vec{V} \rangle) \\ & + \frac{RA_o}{n_R} \sum_R \sum_{\ell,m,n} (\vec{R}_{ijk} - \vec{R}_{\ell mn}) \vec{F}_{ijk;\ell mn} \end{aligned} \tag{4.3}$$

In Eq. (4.1) ρ represents the density, ΔZ_f the (average) final separation along the z axis of the planes which bound the region under consideration, and ΔZ_i the initial separation. The density has been normalized by the initial density. In Eq. (4.2), $\langle \vec{V} \rangle$ is the average velocity and the notation $\sum_R$ denotes that sum was only over atoms in region R; n_R is the number of atoms in that region. Finally the two terms on the right-hand side of Eq. (4.3) represent the kinetic and potential contributions to the pressure or stress tensor $\overleftrightarrow{\sigma}$, respectively. The quantity $\vec{F}_{ijk;\ell mn}$ denotes the force exerted on atom (i,j,k) by atom (ℓ,m,n). The stress has been normalized by the factor $4D/a_o^3$.

In Figure 6 we have plotted the density, the z component of the average velocity, and the zz element of the stress tensor as a function

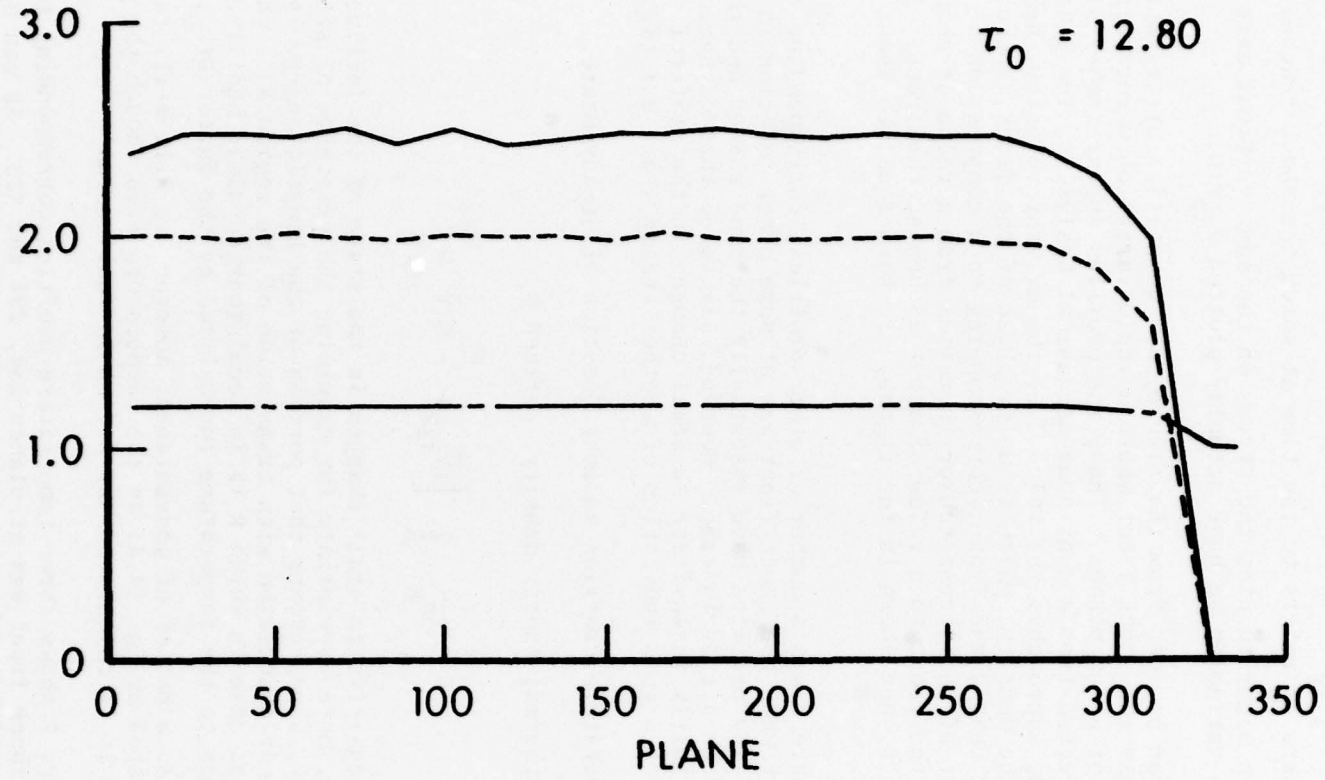

Figure 6. Density, velocity, and stress profiles. Upper curve is $\sigma_{zz}/10$, middle curve $< V_z >$, and lower curve ρ.

of position along the z axis. The values were obtained for the case $U_p=2.0$ for $L_x=L_y=2$ and when the shock was at approximately the 320^{th} plane. Here τ_o refers to the time at which the shock reached that plane. In order to plot the stress on the same vertical axis as the other two variables we have actually plotted $\sigma_{zz}/10$.

As can be seen from the figure, all quantities are rather uniform except near the shock front where a rapid variation occurs within a distance of a few planes. Thus, the profiles appear rather similar to those expected from a continuum-mechanical analysis. The velocity, of course, approaches the value 2.0, the driving velocity, behind the front. The density, which is unity ahead of the front, approaches the value 1.2 behind the front, corresponding to a compression of 20%. The zz element of the stress tensor increases from a value of about 0.5 ahead of the front to a value of about 25 behind the front. The xx and yy elements, not shown in the figure, are both equal to about 20 behind the front.

We have drawn a number of other profiles, corresponding to those above, but when the shock front was at some other location in the lattice. The profiles have essentially the same shapes and therefore appear to be steady in time. However, all three thermodynamic quantities are fairly insensitive to small changes in the state of the lattice and are not a good indication of whether steady state exists.

4.2 Temperature Profiles and the Question of Steady State.

The thermal-energy density, defined by

$$\theta = \frac{1}{3n_R} \sum_R \left[(\vec{V}_{ijk}) - \langle \vec{V} \rangle \right]^2 , \qquad (4.4)$$

is more sensitive to small changes in the state of the lattice and is, therefore, more appropriate for examining the existence of steady state. Physically, θ represents that portion of the kinetic energy in region R which is not associated with translation of the region as a whole. For the special case in which R is in local thermodynamic equilibrium, it corresponds to the temperature (normalized by the factor D/k_B) in the region. As a matter of convenience, however, we will still refer to θ as calculated by Eq. (4.4) as the temperature even though the region for which it is calculated may not be in equilibrium.

Figure 7 shows three temperature profiles corresponding to times when the shock front was at planes 258, 291 and 323. As can be seen from the profiles, the temperature near the front substantially overshoots its final constant value. The overshoot is followed by a region in which thermal relaxation occurs and, finally, a region of nearly

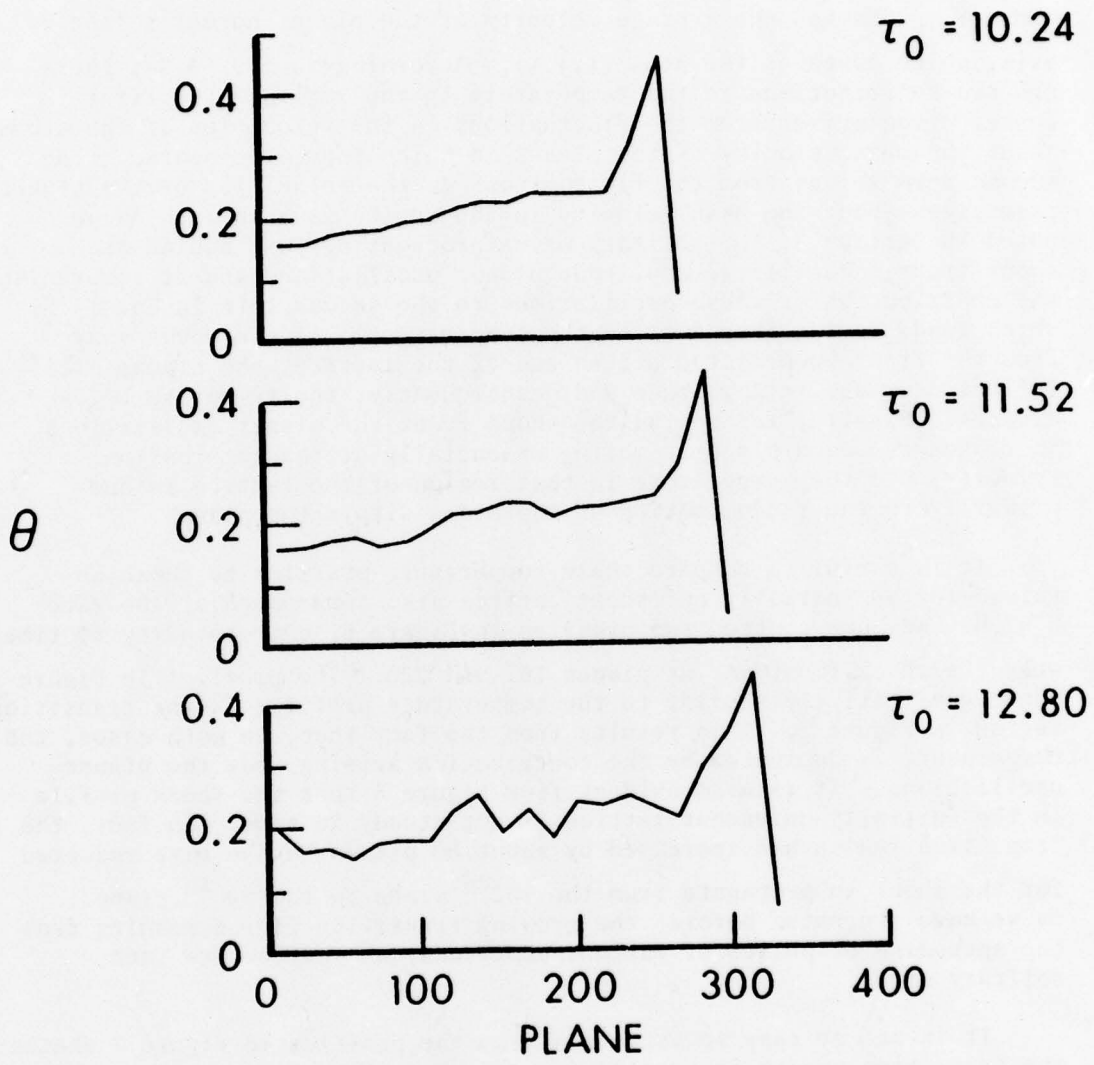

Figure 7. Temperature profiles for the initially thermalized lattice.

constant temperature (roughly, 0.17 or three times ambient). To understand this behavior it is convenient to rewrite Eq. (4.4) as

$$\theta = \frac{1}{3n_R} \sum_R \left[(\vec{V}_{ijk} - \vec{V}^P_{ijk})^2 + (\vec{V}^P_{ijk} - \langle \vec{V} \rangle)^2 \right] \tag{4.5}$$

where $\vec{V}^P_{ijk}$ denotes the average velocity of the plane, normal to the z axis, which contains the atom (i,j,k). According to Eq. (4.5), there are two contributions to the temperature in the region. The first contribution arises from the fluctuations in the velocities of the atoms about the mean velocity of the planes in which they are located. The second term arises from the fluctuations in the velocities of the planes themselves about the mean velocity in the region as a whole. As we noted in Section 3, the solitary waves propagating just behind the shock front induce large-amplitude planar oscillations and it is precisely the contribution of these oscillations to the second term in Eq. (4.5) which leads to the overshoot in the temperature. As one moves away from the front towards the driven end of the lattice, the planar oscillations decrease in amplitude and, consequently, the temperature decreases. Finally, far behind the shock front the planar oscillations have decayed, each plane is moving essentially at the compression velocity, and the temperature in that region of the lattice is due primarily to the random motion of the atoms within the planes.

It is useful to compare these temperature profiles to those obtained for an initially quiescent lattice also compressed at the rate U_p=2.0. We have plotted two profiles in Figure 8, corresponding to times when the shock front was at planes 162 and 226. The profiles in Figure 8 are qualitatively similar to the temperature profiles in the transition region in Figure 7. This results from the fact that, in both cases, the temperature is dominated by the contribution arising from the planar oscillations. It is also evident from Figure 8 that the shock profile in the initially quiescent lattice is not steady in time. In fact, the transition region has increased by about 60 planes in the time required for the shock to propagate from the 162^{nd} plane to the 226^{th} plane. As we have suggested before, the growing transition region results from the spreading of pulses of various amplitude, as they evolve into solitary waves.

It is not so easy to ascertain from the profiles in Figure 7 whether the transition region is growing or not. Unfortunately, thermal background sufficiently obscures the part of the profile resulting from the solitary waves that a spreading effect, if it exists, cannot be unequivocally observed. We have plotted and examined in detail many profiles similar to those in Figure 7 and were unable to come to any conclusion.

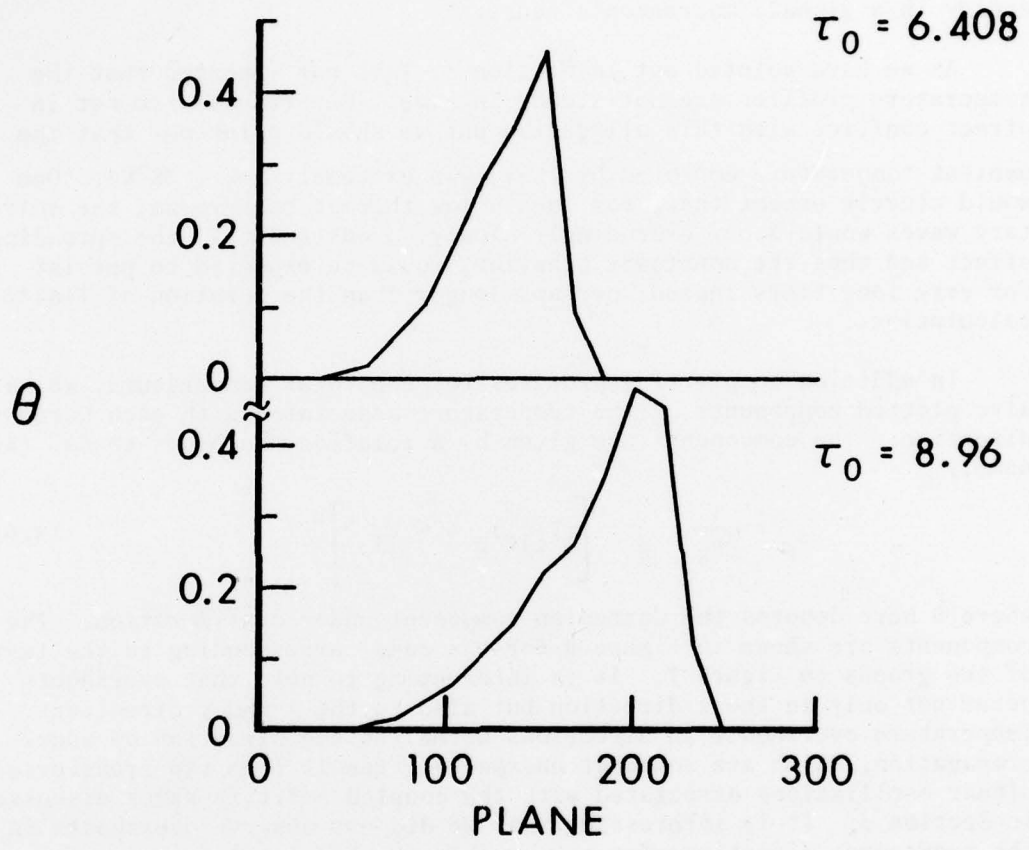

Figure 8. Temperature profiles for the initially quiescent lattice.

We should emphasize that absence of steady state in one dimension and in the three-dimensional quiescent lattice does not necessarily imply that the profile will be unsteady in the three-dimensional, thermalized lattice. The principal difference is that, in the first two cases, there is no appreciable decay of the solitary waves as they propagate into the lattice and the spreading effect must persist. In the last case, however, the solitary waves at the front are not completely stable. Therefore, as they give up their energy to the thermal background and their propagation velocity decreases, they may be overtaken by higher-amplitude solitary waves which were initially behind them. It is then conceivable, if not likely, that such a profile would appear steady in a global, macroscopic sense.

As we have pointed out in Section 1, Tsai has reported that the temperature profiles are not steady in time. Our results are not in direct conflict with this allegation but we should point out that the ambient temperature employed by Tsai[4] was extremely low (~38°K). One would clearly expect that, for such a low thermal background, the solitary waves would decay exceedingly slowly. Consequently, the spreading effect and thus the nonsteady behavior, would be expected to persist for very long times indeed, perhaps longer than the duration of Tsai's calculations.

In addition to plotting profiles for the total temperature, we have also plotted components of the temperature associated with each Cartesian direction. The components are given by a relation analogous to Eq. (4.4), namely

$$\theta_\beta = \frac{1}{3n_R} \sum_R \left[(V_{ijk})_\beta - \langle V_\beta \rangle \right]^2 \qquad (4.6)$$

where β here denotes the Cartesian component under consideration. The components are shown in Figure 9 for the case corresponding to the last of the graphs in Figure 7. It is interesting to note that overshoots occur not only in the z direction but also in the x and y directions. Temperature overshoots in directions normal to the direction of shock propagation, which are somewhat unexpected, result from the transverse planar oscillations associated with the coupled solitary waves discussed in Section 3. It is interesting that we did not observe overshoots in the transverse directions for more weakly shocked lattices, say, for U_p=1.0. We believe that their absence results from the fact that the accompanying longitudinal solitary waves were not sufficiently strong to generate the transverse waves. In fact, we have demonstrated in previous work[22] that there exists a threshold amplitude for the longitudinal solitary wave below which coupled solitary waves do not exist.

4.3 Investigation of Equilibrium.

In the preceding section we have used the term "temperature" rather

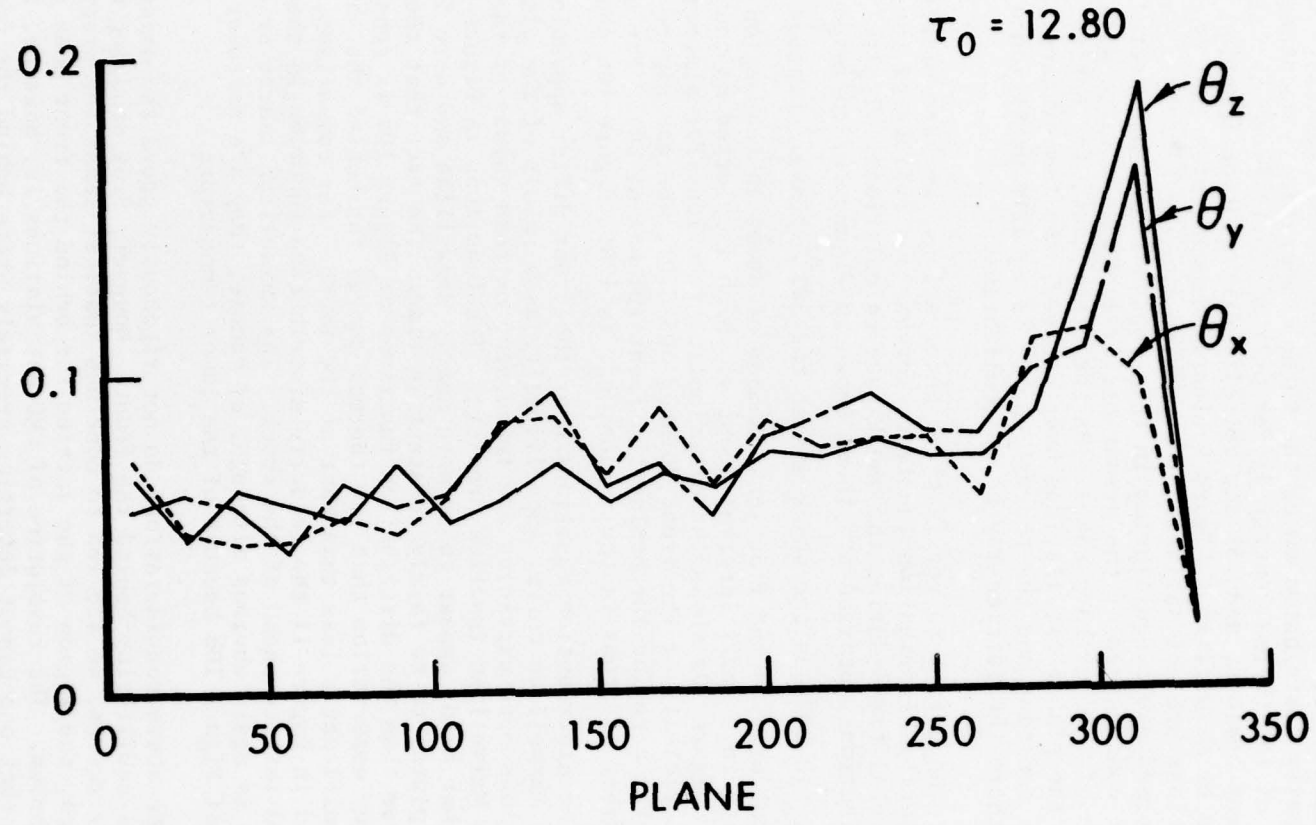

Figure 9. Temperature-component profiles for the initially thermalized lattice.

loosely to denote the nondirected kinetic energy in a region and now we wish to examine the extent to which the region behind the shock is actually in thermal equilibrium. For a region to be in local thermodynamic equilibrium, it is necessary that (1) the thermal energy in the region be equally distributed among the three temperature components, (2) the value of the thermal energy differ only slightly from its value in adjacent regions, and (3) the velocity distribution function in the region be Maxwellian. Figure 9 clearly demonstrates that the first two conditions are not satisfied just behind the shock front. The absence of thermodynamic equilibrium in this region is not unexpected and is a direct consequence of the planar oscillations associated with the propagation of the solitary waves. On the other hand, far behind the front where the planar oscillations have decayed, the temperature is relatively constant and the thermal energy is equally partitioned, suggesting that there the lattice may be in equilibrium.

In an effort to verify these observations, we have plotted a number of velocity distribution functions for various regions of the lattice at several times during the shock-wave calculations. Typical of the distributions obtained are those shown in Figure 10, corresponding to time τ_o=12.80 when the shock was at the 323rd plane. Plotted on the vertical axis is the fractional number of atoms in the region having velocity in a small interval about V, which is plotted on the horizontal axis. Figure 10a shows the distribution functions for sixteen planes in the vicinity of the front (planes 305-320), whereas Figure 10b shows those for a region far behind the front (planes 65-80). For each sample the number of atoms in the region, n_R, is 128. Figure 10a shows clearly that the distribution functions near the front differ appreciably from a true Maxwellian curve. Specifically, as a result of the planar oscillations more particles are found near extreme values of the velocity than a Maxwellian function predicts. The functions in Figure 10b, on the other hand, appear to be more nearly Maxwellian and were found, from other plots, to be fairly constant in time. The fact that they are much narrower than the distribution functions of Figure 10a is consistent with our observation that the thermal energy far behind the shock front is significantly less than that at the front. For comparison, we have plotted in Figure 11 the velocity distribution function in the uncompressed lattice ahead of the shock. The Maxwellian character of these curves is again obvious although, of course, they are narrower than those of Figure 10b because of the lower temperature.

The above considerations do not rigorously prove the existence of thermal equilibrium behind the front. However, from studying many similar curves, we are led to conclude that, at least for practical purposes, the region of the lattice far behind the front does approach equilibrium. The resolution of CMD calculations is, however, limited enough that one cannot determine precisely where behind the front thermal equilibrium is first re-established. Consequently, we are unable to determine conclusively from our calculations if the region of thermal equilibrium lags behind the shock front, as claimed by Tsai.

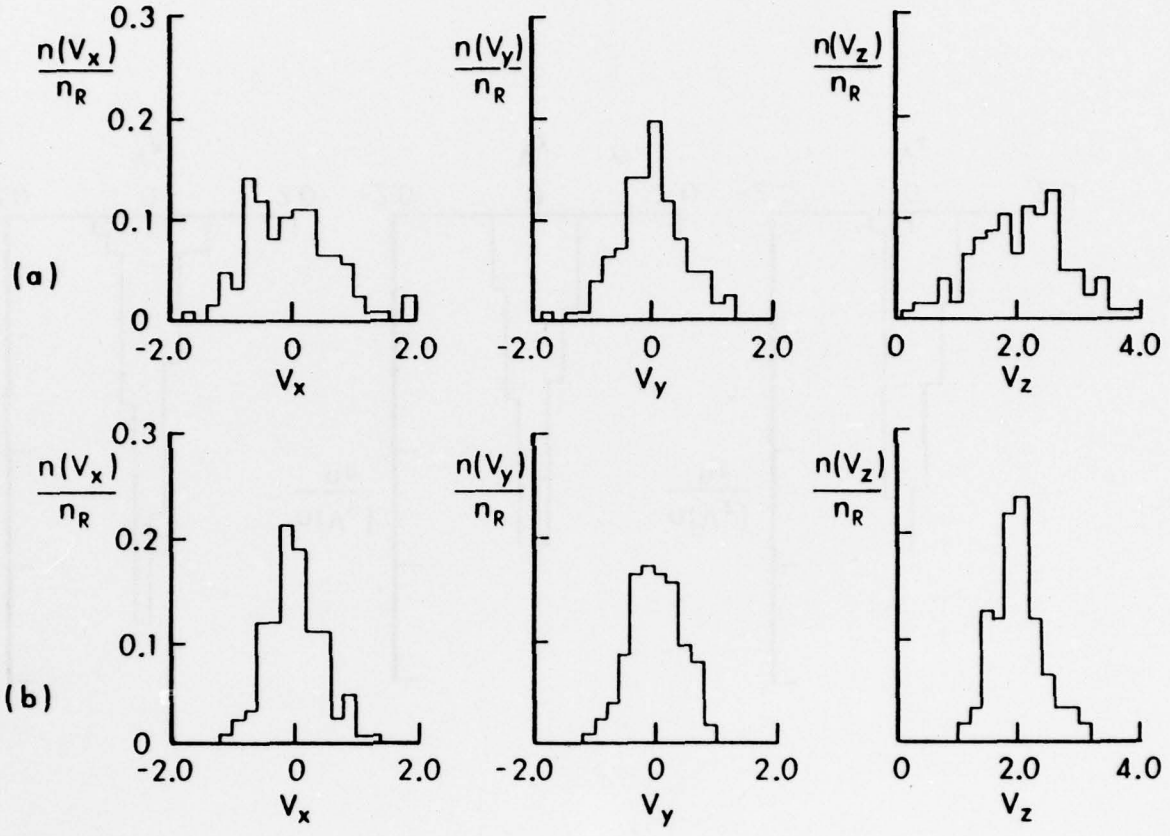

Figure 10. Velocity distribution functions. (a) Planes 305-320. (b) Planes 65-80.

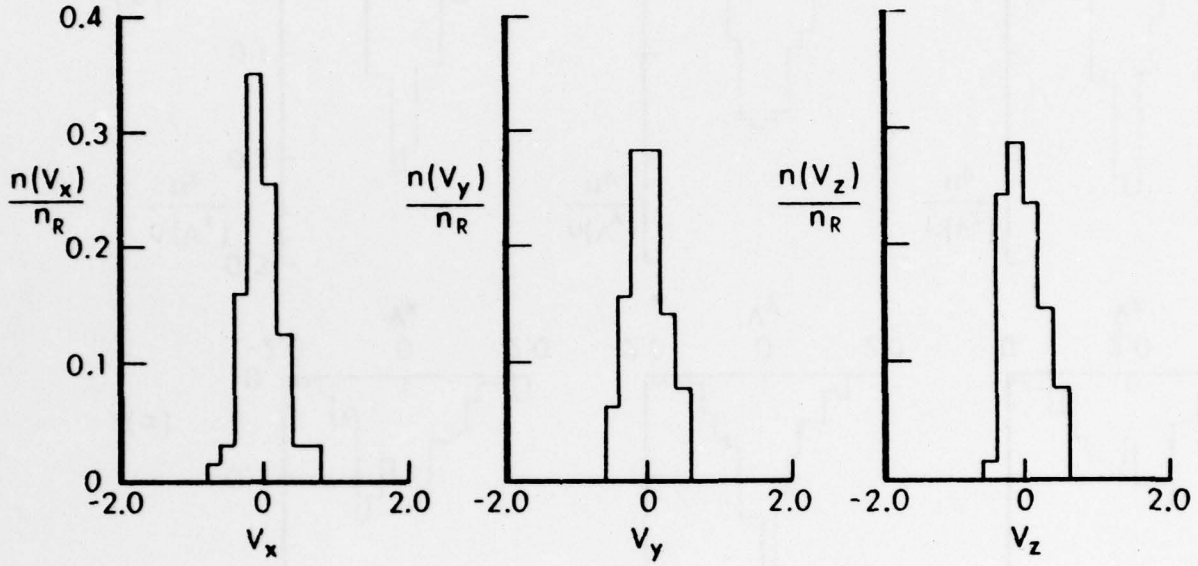

Figure 11. Velocity distribution function in uncompressed lattice.

5. DISCUSSION

In this final section we will be concerned primarily with summarizing the results of our calculations, discussing the limitations of the model, and comparing our conclusions with those reached by other investigators. We will also indicate the relevance of our work to other Army-related problems as well as suggest possible future applications of CMD techniques.

To re-emphasize, we believe that shock propagation in the three-dimensional discrete lattice occurs in the following manner. Steady compression gives rise to a spectrum of longitudinal solitary waves which propagate in the vicinity of the shock front and continuously interact with the thermal background of the lattice. The longitudinal waves accentuate transverse planar oscillations and can, if sufficiently strong, produce coupled longitudinal-transverse solitary waves. The existence of both types of solitary waves is made evident by the temperature overshoots which occur in all three Cartesian directions for strong shocks.

The propagation velocity of the solitary waves increases with increasing amplitude and, thus, they tend to spread apart as they propagate. At least for early times this spreading effect results in a growing transition region behind the front. If the solitary waves were stable in three dimensions, as they were in our one-dimensional calculations, the spreading effect would persist and a steady profile could not exist. The lack of absolute stability in three dimensions, however, leads to the distinct possibility that the profile will become steady in a macroscopic sense in the long-time limit. Unfortunately, our data are not sufficient to settle the question conclusively for the times for which we ran the calculations, and the limitations of the CMD technique preclude longer calculations.

Despite the fact that considerable information can be learned from CMD shock-wave studies, we should point out that caution in interpreting the results should always be exercised. The most obvious limitation of the method is the inability to propagate the shock front macroscopic distances into the lattice. This limitation has, for instance, precluded a more careful examination of the question of steady state and the approach to equilibrium behind the front. A second major limitation of the method is the inability to treat lattices having reasonably large cross sections. It is possible, therefore, that phenomena which occur in CMD simulations may be a direct consequence of the small cross sections used and may not occur in systems with more realistic transverse dimensions. For example, in the present calculations the number of atoms in a plane is sufficiently small (32, at most) that the average planar velocity will not be zero even in the initial thermal background. Interaction of the longitudinal solitary wave with these background planar oscillations enhances the decay of the solitary waves and, in some cases, leads to the generation of coupled longitudinal - transverse

solitary waves. As the number of particles in the cross section is increased, the amplitude of the planar velocity in the thermal background is decreased. Therefore, in a crystal having a considerably larger cross section the longitudinal solitary waves may in fact be more stable than those observed here, and the appearance of coupled solitary waves, if it occurs at all, will be significantly delayed. In spite of the deficiencies, we believe that CMD calculations provide a reasonable qualitative picture of what happens in real solids subjected to shock compression. In looking at details, however, one must be exceedingly careful and for this reason we are unable to provide a definite answer to the question of whether or not the shock profile is steady.

We would now like to turn our discussion to the definition of temperature behind the shock front and, hopefully, to shed some light upon a controversy between Tsai[4,6] and Paskin that has existed in the literature for some time. The disagreement arises only over the z component of the temperature. To determin this quantity, Paskin[11] first defines the z component of the planar temperature by

$$(\theta_1)_z = \frac{1}{3n_p} \sum_p \left[(V_{ijk})_z - \langle V_z \rangle \right]^2 \tag{5.1}$$

where the sum extends only over atoms in a particular plane normal to the z axis. Thus, n_p is the number of atoms in the plane and $\langle V_z \rangle$ represents the average instantaneous velocity of the plane in the z direction. The z component of the temperature in a region is then obtained by averaging $(\theta_1)_z$ over the planes in the region. Presumably, the rationale for this perhaps unusual definition is that one thereby does not consider the energy associated with the planar oscillations near the front as part of the random thermal energy or temperature. Tsai, on the other hand, has insisted upon using the definition

$$(\theta_2)_z = \frac{1}{3n_R} \sum_R \left[(V_{ijk})_z - U_p \right]^2 \tag{5.2}$$

where the sum now extends not only over atoms in a given plane, but also over many planes (i.e., making up a region R). We, for comparison, have employed the definition

$$\theta_z = \frac{1}{3n_R} \sum_R \left[(V_{ijk})_z - \langle V_z \rangle \right]^2 \tag{5.3}$$

where $\langle V_z \rangle$ here represents the actual average velocity in the region under consideration.

The first point we wish to make is that none of the above three definitions is "wrong". Since temperature has a precise meaning only in the context of equilibrium statistical mechanics, one is free to define it arbitrarily in the nonequilibrium region behind the shock provided the definition reduces to the standard one in equilibrium. All three definitions satisfy this criterion so the only point open to discussion is which definition is the most reasonable.

Tsai's definition of temperature is essentially the same as ours except that Tsai has assumed that the translational velocity behind the shock is everywhere given by the compression velocity U_p. The reason that he has chosen to use this value rather than to calculate the actual average velocity in the region considered is not clear, but apparently he believes that the compression velocity is achieved almost immediately behind the front. Our results do not entirely substantiate this belief. We found, for instance, that when the shock was at the 323^{rd} plane (see Figure 6), the average value of V_z calculated between planes 305 and 320 was 1.57 and between planes 289 and 304 was 1.83. Both these values are significantly less then the final equilibrated value of 2.0 attained still farther behind the front. The use of U_p rather than $< V_z >$ in the definition of temperature would lead to a higher temperature overshoot in Tsai's profiles than in ours.

The principal conceptual difference in the three definitions, however, is whether to include the planar oscillations as thermal energy (as Tsai and we choose to do) or as mean flow energy (as Paskin does). The choice significantly affects the temperature profile since the overshoot at the shock front disappears if the planar oscillations are not included in the definition of the temperature. Actually, the issue is moot and one can make an argument for either choice. Since the planar oscillations are coherent, well-defined waveforms, they do not, in fact, represent the random motion ordinarily associated with thermal energy. On the other hand, the planar oscillations are sufficiently narrow that there is a substantial difference in the velocity of adjacent planes. The oscillations, therefore, contribute significantly to the relative velocities of atoms in adjacent planes and, in that sense, have an effect similar to random thermal motion. In any case, we feel that it is more important to understand why the interplanar oscillations arise and how they might affect the properties of the crystal than to attempt to categorize them.

A major objective of studying shock propagation in discrete lattices is to determine how the results compare with more standard continuum-mechanical calculations. These considerations are important to a number of Army-related problems, particularly detonation, as we have discussed in Reference 1. Currently used theories of shock-induced detonation, for instance, are based on the assumption that the details

of the shock front can be ignored. Thus, the only function of the shock is to raise the temperature, density and pressure of the solid behind the shock front to values higher than ambient. Chemical reactions are then assumed to occur in the high-temperature, thermally equilibrated region behind the shock.

In the present calculations, however, we have found that there exists a sizable, if not growing, region immediately behind the front which is far removed from thermal equilibrium. It would be desirable to determine how such a region of nonequilibrium would affect chemical-reaction rates. Unfortunately, the question is difficult to answer because very little is known about chemical reactions in solids, and less still about how the rates are affected by conditions of non-equilibrium. Nevertheless, it seems reasonable to speculate that reactions are more likely to occur in regions of the lattice where both the thermal and potential energies of the atoms are high.

Therefore, to estimate very roughly the likelihood of reactions, we have plotted in Figure 12 the sum of the potential and thermal energies behind the shock. The thermal energy has been obtained from Eq. (5.3) except that, instead of averaging over 16 planes to calculate θ, we first averaged over only two planes, obtained the appropriate θ, and then averaged the result over 8 consecutive sets of two planes. The purpose of performing the average in this manner is to retain only that portion of the planar oscillations which leads to relative motion of atoms in adjacent planes, which are the most likely to react. We did find, however, that performing the average in this manner led to results similar to those obtained by simply averaging over 16 planes in Eq. (5.3) except that the temperature overshoot at the shock front was reduced by approximately 15%. This relatively small decrease in the temperature at the front indicates that, at least for this case, the width of the solitary waves is of the same order of magnitude as the interatomic separation. In fact, it is easy to verify from the planar trajectories that the solitary waves near the front extend over approximately three lattice planes.

The quantity e' plotted in Figure 12 represents the average thermal and potential energy per particle in regions of the lattice containing 16 planes along the z axis. The temperature was calculated in the manner discussed above and is related to the thermal energy by the relation

$$E_{TH} = 3/2\ n_R\ \theta; \tag{5.4}$$

the zero-point potential, or potential of the uncompressed, quiescent lattice was also subtracted from the definition of e'. Therefore, e' was given by the relation

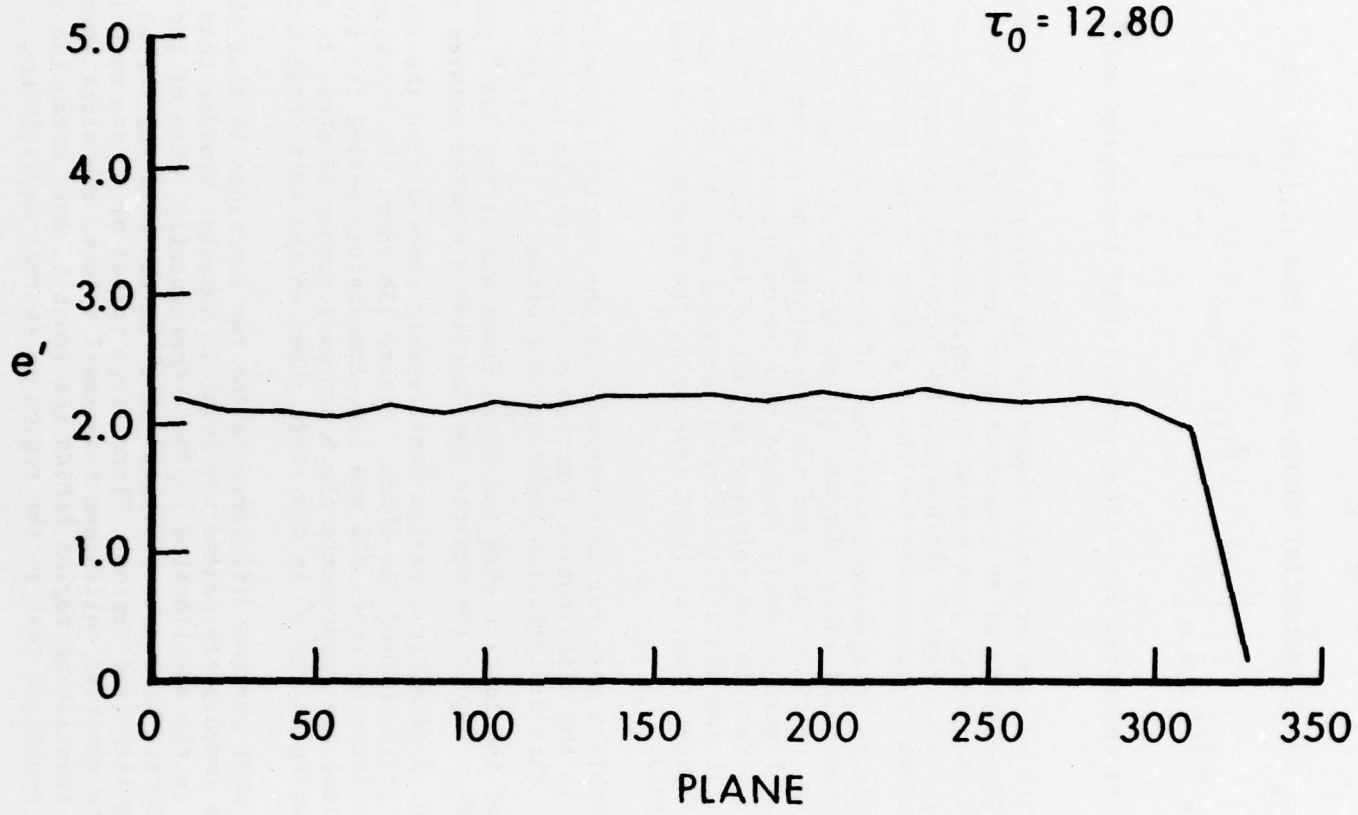

Figure 12. Sum of potential and thermal energies per particle as a function of position behind the shock.

$$e' = 3/2\ \theta + \frac{1}{n_R} \sum_{R} \Phi_{ijk} - \frac{1}{n_R}\ \Phi^{(0)} \qquad (5.5)$$

where Φ_{ijk} is the potential energy of the atom (i,j,k), viz.,

$$\Phi_{ijk} = 1/2 \sum_{\ell,m,n} \left[e^{-R(A_o|\ \vec{R}_{ijk} - \vec{R}_{\ell mn}\ |-1)} - 1 \right]^2 , \qquad (5.6)$$

and $\Phi^{(0)}$ is the total zero-point potential of the region under consideration.

As can be seen from the figure, e' is fairly constant behind the shock. The absence of an overshoot in e' results from the fact that the potential energy just behind the shock front is lower than it is in the equilibrated region far behind the front and, in fact, the difference is sufficient to compensate for the overshoot in the thermal energy. This result is in agreement with that of Paskin[11] who found no overshoot in the total energy density behind the shock. Therefore, if only e' were the relevant parameter for determining the probability of reactions, Figure 12 would suggest that reactions are equally probable in the equilibrated and relaxing regions of the lattice. The assumption that equilibrium was attained immediately behind the front would perhaps be satisfactory then, at least insofar as the chemistry of the problem is concerned.

Probably a more reliable estimate of the reaction probability, however, is the distribution function of e' at various positions in the lattice. This distribution function is plotted in Figure 13 for two regions of the lattice when the shock front was at the 323rd plane (τ_o=12.80). Figure 13a depicts the function evaluated between planes 65 and 80, presumably a region considerably removed from the thermally relaxing region behind the shock. Figure 13b shows the function evaluated between planes 305 and 320, immediately behind the front. The vertical axis represents the fractional number of atoms in the region having energy e' in the range shown on the horizontal axis.

The most obvious difference in the two functions is that the distribution immediately behind the front is somewhat broader than that obtained in the equilibrated region. Consequently, more of the atoms in the lattice have extreme values of e' in the relaxing region than in the equilibrated region. Since large values of e' are more likely to lead to reactive collisions than small values, one might speculate that the transistion region behind the front is more conducive to chemical reactions than is the region in thermal equilibrium.

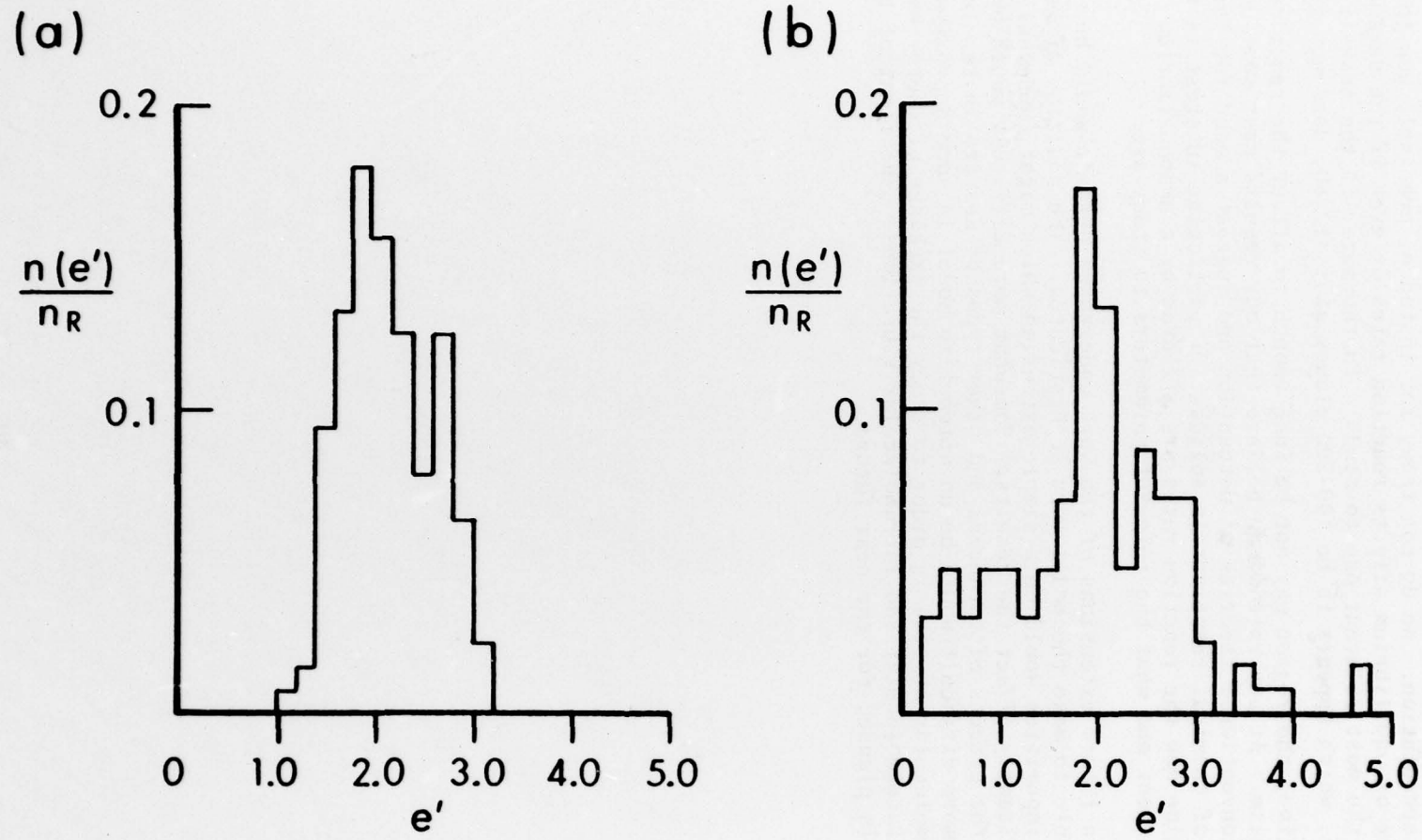

Figure 13. Distribution function for the sum of the thermal and potential energies per particle. (a) Planes 65-80. (b) Planes 305-320.

The above analysis is decidedly imprecise and is intended only as crude speculation. We do not know, for instance, precisely how the absence of equilibrium affects reaction rates or even if the parameter e' is the most relevant one to study. Furthermore, if the transition region, which appears to be 100-200 planes at τ_0=12.80, does not grow with time, the region may not be long enough to affect the reaction mechanism. At any rate we do believe that our results cast some doubt upon conventional theories of detonation and suggest a need for further study of chemical reactions in solids. Of particular interest is to determine how the reaction rates are affected by a nonequilibrium environment and what the relevant parameters to study are.

In future extensions of the work undertaken here it would be desirable to make the model more sophisticated. The addition of isotopic impurities would be a simple extension which might, nonetheless, significantly affect the results. Somewhat more difficult would be to treat the effects of vacancies and other types of defects in the lattice. Still more difficult would be an attempt to model in some approximate way a molecular crystal in order to study the exchange of energy between intermolecular and intramolecular vibrations. The first of these tasks is planned for the near future.

REFERENCES

1. J.D. Powell and J.H. Batteh, "Shock Propagation in the One-Dimensional Lattice", BRL Report No. 2009, US Army Ballistic Research Laboratories, Aberdeen Proving Ground, MD, 1977. See also J.H. Batteh and J.D. Powell, "Shock Propagation in the One-Dimensional Lattice at Nonzero Initial Temperature", J. Appl. Phys. 49, 3933 (1978) and J.H. Batteh and J.D. Powell, in Solitons in Action, edited by K. Lonngren and A. Scott (Academic Press, New York, 1978, p. 257.

2. B.J. Alder and T.E. Wainwright, "Studies in Molecular Dynamics. I. General Method", J. Chem. Phys. 31, 459 (1959).

3. J.D. Powell and J.H. Batteh, "Shock Propagation in the Three-Dimensional Lattice. II. Method of Calculation", BRL Report (to be published concurrently with this report).

4. R.A. MacDonald and D.H. Tsai, "Molecular Dynamical Calculations of Energy Transport in Crystalline Solids", Phys. Reports 46, 1 (1978).

5. D.H. Tsai and C.W. Beckett, "Shock Wave Propagation in Cubic Lattices", J. Geophys. Res. 71, 2601 (1966).

6. D.H. Tsai and R.A. MacDonald, "Second Sound in a Solid Under Shock Compression", J. Phys. C 6, L171 (1973).

7. J.C. Ward and J. Wilks, "Second Sound and the Thermo-Mechanical Effect at Very Low Temperatures", Phil. Mag. 43, 48 (1952).

8. M. Chester, "Second Sound in Solids", Phys. Rev. 131, 2013 (1963).

9. A. Paskin and G.J. Dienes, "Molecular Dynamic Simulations of Shock Waves in a Three-Dimensional Solid", J. Appl. Phys. 43, 1605 (1972).

10. A. Paskin and G.J. Dienes, "A Model for Shock Waves in Solids and Evidence for a Thermal Catastrophe", Solid State Comm. 17, 197 (1975).

11. A. Paskin, A. Gohar, and G.J. Dienes, "Simulations of Shock Waves in Solids", J. Phys. C 10, L563 (1977).

12. J. Tasi, "Perturbation Solution for Growth of Nonlinear Shock Waves in a Lattice", J. Appl. Phys. 43, 4016 (1972). See also Erratum [J. Appl. Phys. 44, 1414 (1973)].

13. J. Tasi, "Perturbation Solution for Shock Waves in a Dissipative Lattice", J. Appl. Phys. 44, 2245 (1973).

14. J. Tasi, "Far-Field Analysis of Nonlinear Shock Waves in a Lattice", J. Appl. Phys. 44, 4569 (1973).

15. G.E. Duvall, R. Manvi, and S.C. Lowell, "Steady Shock Profile in a One-Dimensional Lattice", J. Appl. Phys. 40, 3771 (1969).

16. R. Manvi, G.E. Duvall, and S.C. Lowell, "Finite Amplitude Longitudinal Waves in Lattices", Int. J. Mech. Sci. 11, 1 (1969).

17. R. Manvi and G.E. Duvall, "Shock Waves in a One-Dimensional, Non-Dissipating Lattice", Brit. J. Appl. Phys. 2, 1389 (1969).

18. J.R. Hardy and A.M. Karo, "Theoretical Studies of Soliton-Like Behavior of Shocks in One-Dimensional Systems", LLL Report No. UCRL-79259, Lawrence Livermore Laboratory, Livermore, CA, 1977.

19. B.L. Holian and G.K. Straub, "Molecular Dynamics of Shock Waves in One-Dimensional Chains", Phys. Rev. B 18, 1593 (1978).

20. N.J. Zabusky and M.D. Kruskal, "Interaction of Solitons in a Collisionless Plasma and the Recurrence of Initial States", Phys. Rev. Letters 15, 240 (1965).

21. F. Milstein, "Applicability of Exponentially Attractive and Repulsive Interatomic Potential Functions in the Description of Cubic Crystals", J. Appl. Phys. 44, 3825 (1973).

22. J.H. Batteh and J.D. Powell, "Solitary-Wave Propagation in the Three-Dimensional Lattice", Phys. Rev. B (in press).

DISTRIBUTION LIST

No. of Copies	Organization
12	Commander Defense Documentation Center ATTN: DDC-DDA Cameron Station Alexandria, VA 22314
1	Commander US Army Materiel Development and Readiness Command ATTN: DRCDMD-ST 5001 Eisenhower Avenue Alexandria, VA 22333
1	Commander US Army Aviation Research and Development Command ATTN: DRSAV-E P.O. Box 209 St. Louis, MO 63166
1	Director US Army Air Mobility Research and Development Laboratory Ames Research Center Moffett Field, CA 94035
1	Commander US Army Electronics Research and Development Command Technical Support Activity ATTN: DELSD-L Fort Monmouth, NJ 07703
1	Commander US Army Communications Rsch and Development Command ATTN: DRDCO-PPA-SA Fort Monmouth, NJ 07703
2	Commander US Army Missile Research and Development Command ATTN: DRDMI-R DRDMI-YDL Redstone Arsenal, AL 35809
1	Commander US Army Tank Automotive Rsch and Development Command ATTN: DRDTA-UL Warren, MI 48090
2	Commander US Army Armament Research and Development Command ATTN: DRDAR-TSS (2 cys) Dover, NJ 07801
1	Commander US Army Armament Materiel Readiness Command ATTN: DRSAR-LEP-L, Tech Lib Rock Island, IL 61299
2	Commander US Army Armament Research and Development Command ATTN: DRDAR-LCN, Dr. P. Harris DRDAR-LCE, Dr. F. Owens Dover, NJ 07801
1	Director Army Materials & Mechanics Research Center ATTN: Dr. R. Harrison Watertown, MA 02172
1	Director US Army TRADOC Systems Analysis Activity ATTN: ATAA-SL, Tech Lib White Sands Missile Range, NM 88002
3	Commander US Army Research Office ATTN: Dr. M. Ciftan Dr. E. Saibel Dr. J. Chandra P.O. Box 12211 Research Triangle Park, NC 27709

DISTRIBUTION LIST

No. of Copies	Organization
1	Commander Army Research & Standardization (Group) Europe Electronics Branch Dr. Alfred K. Nedoluha Box 65 FPO, NY, NY 09510
1	Director Naval Surface Weapons Center ATTN: Dr. D.J. Pastine White Oak, MD 20910
6	Director Lawrence Livermore Laboratory ATTN: Dr. W. Hoover, Dr. A. Karo Dr. C.M. Tarver, Dr. E.L. Lee, Dr. W. VonHolle, Dr. F.E. Walker Livermore, CA 94550
2	Director Los Alamos Scientific Lab ATTN: Dr. B.L. Holian Dr. G.K. Straub Los Alamos, NM 87544
3	Director National Bureau of Standards ATTN: Dr. H. Prask Dr. S. Trevino Dr. D. Tsai Gaithersburg, MD 20760
1	Director NASA Goddard Space Flight Ctr Mail Code 624 ATTN: Dr. J.E. Allen Greenbelt, MD 20771
1	Science Applications, Inc. ATTN: Mr. S. Howie 6600 Powers Ferry Rd, Suite 220 Atlanta, GA 30339
1	City College of New York Department of Physics ATTN: Professor M. Lax 138th St. & Convent Ave. New York, NY 10031
1	Massachusetts Institute of Technology Dept. of Nuclear Engineering ATTN: Professor S. Yip Cambridge, MA 02139
1	Princeton University Astrophysics Department Professor M.D. Kruskal Princeton, NJ 08540
1	Queens College ATTN: Professor A. Paskin Flushing, NY 11973
1	State University of New York Department of Mechanics ATTN: Professor J. Tasi Stony Brook, NY 11790
2	University of Arizona Department of Mathematics ATTN: Dr. D. McLaughlin Dr. H. Flaschka Tucson, AZ 85721
1	University of California at Irvine Department of Physics ATTN: Dr. A. Maradudin Irvine, CA 92664
1	University of Delaware Department of Physics ATTN: Prof. Fred Williams Newark, DE 19711

DISTRIBUTION LIST

No. of Copies	Organization
2	University of Florida Department of Engineering ATTN: Prof. K.T. Millsaps Prof. B.M. Leadon Gainesville, FL 32603
2	University of Florida Department of Physics and Astronomy ATTN: Prof. J.W. Dufty Prof. C.F. Hooper Gainesville, FL 32603
1	University of Massachusetts Department of Physics ATTN: Professor R. Guyer Amherst, MA 01002
1	University of Nebraska ATTN: Professor J.R. Hardy Lincoln, NE 68588
1	University of Pittsburgh ATTN: Prof. N.J. Zabusky Pittsburgh, PA 15260
1	University of Rochester Department of Physics and Astronomy ATTN: Professor E. Montroll Rochester, NY 14627
1	University of Tennessee Space Institute ATTN: Prof. D.R. Keefer Tullahoma, TN 37388
1	University of Wisconsin Department of Electrical and Computer Engineering ATTN: Prof. A. Scott Madison, WI 53706
1	Washington State University Shock Dynamics Laboratory ATTN: Prof. G. Duvall Pullman, WA 99163

Aberdeen Proving Ground

Dir, USAMSAA
ATT: Dr. J. Sperrazza
DRXSY-MP, H. Cohen
Cdr, USATECOM
ATTN: DRSTE-TO-F
Dir, Wpns Sys Concepts Team,
Bldg. E3516, EA
ATTN: DRDAR-ACW